scientific reports

Check for updates

OPEN

Autophagy-related biomarkers identified in sepsis-induced ARDS through bioinformatics analysis

Wei Wang, Jianfeng Zhao, Hui Li, Dabing Huang, Shuiqiao Fu✉ & Zhitao Li✉

While dysregulated autophagy has been linked to acute respiratory distress syndrome (ARDS) development in sepsis, the exact regulatory mechanisms driving this process remain unclear. This study systematically investigated autophagy-related genes in sepsis-induced ARDS using integrative bioinformatics, including weighted gene coexpression network analysis (WGCNA), differential gene expression analysis (DEGs), receiver operating characteristic (ROC) curve analysis, Gene Ontology (GO) and Kyoto Encyclopedia of Genes and Genomes (KEGG) enrichment analysis, protein–protein interaction (PPI) network analysis, and immune infiltration analysis. Hub genes were further validated by qPCR in Beas-2B cells receiving lipopolysaccharide (LPS) stimulation. We identified 18 autophagy-related DEGs with diagnostic potential for sepsis-induced ARDS. These DEGs were linked to endocytosis, protein kinase inhibition, and enigmatic Ficolin-1-rich granules. The downregulated hallmark signaling pathways involved apoptosis, complement, IL-2/STAT5, and KRAS signaling. Immune infiltration analysis revealed alterations in 7 immune cell subsets, including CD8 + T-cell exhaustion, natural killer cell reduction, and the type 1 helper T-cell response. When Beas-2B cells were treated with LPS, we discovered that 6 out of the 18 hub genes were significantly downregulated. Our findings provide novel insights into autophagy-mediated ARDS pathogenesis in sepsis. The hub genes represent promising candidates for clinical biomarker development and therapeutic targeting, which necessitates further validation.

Keywords Autophagy, Acute respiratory distress syndrome, Sepsis, Bioinformatics

Sepsis is a life-threatening dysfunction of organs caused by an unregulated host response to infection[1]. Acute respiratory distress syndrome (ARDS) is considered one of the earliest and most prevalent complications of sepsis, with a prevalence ranging from 6 to 30%[2–8]. ARDS significantly increases in-hospital mortality in these patients[2,5,6].

ARDS and sepsis share overlapping pathophysiological mechanisms[9], characterized by three interconnected pathological processes: (1) pulmonary inflammatory storm marked by uncontrolled cytokine release and oxidative stress, (2) microcirculatory failure stemming from glycocalyx disruption, mitochondrial dysfunction, and coagulopathy, and (3) programmed cell death activation involving apoptosis, necrosis, pyroptosis, and autophagy-related cytotoxicity[10].

Notably, emerging evidence highlights autophagy's important role in sepsis-induced ARDS[11–15]. This evolutionarily conserved process maintains cellular homeostasis through organelle recycling[16] and modulates immune responses via pathogen clearance and inflammation regulation[17]. However, its precise role in ARDS pathogenesis remains controversial. Autophagy can provide cytoprotection by degrading damaged organelles or misfolded proteins, whereas in cases involving indigestible stimuli such as viruses, autophagy may interact with the endocytosis and exosome pathways to mediate cellular cytotoxicity[18].

This study aims to clarify how autophagy-related genes contribute to sepsis-induced ARDS using bioinformatics to identify key genes and pathways. The findings may aid in developing new diagnostic and therapeutic strategies for sepsis-induced ARDS, enhancing patient care.

Methods

Data acquisition

The data utilized in this study are publicly available from the Gene Expression Omnibus (GEO) (https://www.ncbi.nlm.nih.gov/geo/). The analysis included two datasets: GSE10474 (13 sepsis-induced ARDS patients vs.

Department of Surgical Intensive Care Unit, First Affiliated Hospital, School of Medicine, Zhejiang University, 79 Qingchun Road, Hangzhou 310003, China. ✉email: 2200048@zju.edu.cn; lizhitao402@163.com

21 sepsis controls) and GSE32707 (31 sepsis-induced ARDS patients vs. 58 sepsis controls). Whole-genome expression profiles were acquired using the "GEO query" R package (version 2.70.0), followed by batch effect correction with the ComBat algorithm implemented in the "sva" R package (version 3.50.0).

The autophagy-related genes were curated from two established databases: the Human Autophagy Moderator Database (HAMdb, hamdb.scbdd.com) and the Human Autophagy Database (HADb, www.autophagy.lu). This comprehensive curation process identified 803 unique autophagy-associated genes for downstream analysis.

Weighted gene coexpression network analysis (WGCNA) and identification of the autophagy-related module

We performed WGCNA using the R package WGCNA (version 1.70-3). Gene expression profile similarities were assessed using Pearson correlation analysis. We optimized network connectivity using a power β value (soft-thresholding) to achieve scale-free topology ($R^2 > 0.85$). Hierarchical clustering with dynamic tree cutting (minimum module size = 30 genes) identified distinct co-expression modules, each color-coded for visualization. Cluster stability was validated through topological overlap matrix (TOM)-based dissimilarity measures. To identify the module significantly associated with autophagy, we calculated Pearson correlations between module eigengenes (MEs) and autophagy. We visualized the coexpression module structure with a heatmap of gene network topology overlap and summarized module relationships through hierarchical clustering and a corresponding feature vector heatmap.

Autophagy-related differentially expressed genes (DEGs) in sepsis-induced ARDS

The R package "limma (version 3.50.0)" was utilized to identify DEGs between the sepsis-induced ARDS group ($n = 44$) and the control group (sepsis alone, $n = 79$). The screening criteria applied were a $|\log2\text{-fold change}| > 0.5$ and a P value < 0.05. Additionally, the R package "pheatmap" was employed to generate heatmaps, and Euclidean distance and hierarchical clustering methods were used for clustering purposes. Autophagy-related DEGs were identified by intersecting DEGs with autophagy-related module genes derived from WGCNA.

Receiver operating characteristic (ROC) curve

We utilized the R package "pROC" to create ROC curves and calculate the corresponding area under the curve (AUC) to assess the diagnostic value of the hub genes for sepsis-induced ARDS.

Gene ontology (GO) and Kyoto encyclopedia of genes and genomes (KEGG)

We utilized the R package "clusterProfiler (version 4.2.2)" to conduct GO analysis and KEGG pathway enrichment analysis for DEGs related to autophagy ($P < 0.05$).

Protein–protein interaction (PPI) analysis

A PPI network for the hub genes was constructed using the GeneMANIA website (http://genemania.org).

Comparison of HALLMARK signaling pathways

We obtained 50 HALLMARK signaling pathways in symbol format from the Molecular Signatures Database (MSigDB) and calculated Gene Set Variation Analysis (GSVA) scores for each pathway in every sample using the single-sample Gene Set Enrichment Analysis (ssGSEA) method. Subsequently, we compared the GSVA scores of different HALLMARK signaling pathways between the two groups using the Limma package (version 3.58.1). Furthermore, we conducted a correlation analysis between the top five autophagy-related DEGs and the 50 HALLMARK signaling pathways.

Immune infiltration analysis

We performed ssGSEA to calculate the enrichment scores of various immune cell types for each sample. This analysis was based on data from the Tumor and Immune System Interaction Database (TISIDB) (http://cis.hku.hk/TISIDB/index.php). Subsequently, we visualized the changes in immune cell infiltration levels between the sepsis-induced ARDS group and the control group using the R package "ggplot2" (version 3.3.6).

Hub gene expression in beas-2B cells

The impact of autophagy on pulmonary epithelial cells in sepsis was explored by treating Beas-2B cells with or without 1 μg/ml LPS. Total RNA was isolated from Beas-2B cells using the TRIzol reagent (AB & Invitrogen, USA) according to the manufacturer's instructions. The concentration and purity of the RNA were measured using a spectrophotometer. cDNA synthesis was performed using 1.0 μg of total RNA and the SureScript First-strand cDNA synthesis kit (GeneCopoeia, Guangzhou) according to the kit protocol. The cDNA was then subjected to real-time PCR using the iQ SYBR Green Supermix (Kapa Biosystems, USA) on a Light Cycler 480 System (Roche, Switzerland) following the manufacturer's instructions. The expression levels of the target gene were evaluated using the 2-ΔΔCt method, with GAPDH as the internal control. The qPCR primers were designed by Qingke Biology Co., Ltd. (listed in the Supplementary Material 1).

Statistical analysis

Statistical analysis was performed using R software version 4.1.2. The Spearman correlation test was employed to assess the correlation between two parameters. The Wilcoxon test was utilized to compare differences between two groups, and the Kruskal–Wallis test was applied to evaluate differences among three or more groups. A two-sided P value of less than 0.05 was considered indicative of statistical significance.

Results

WGCNA and identification of the Autophagy-Related module

The assessment of scale independence and average connectivity indicated that a soft threshold (β) of 7 was optimal, resulting in an average connectivity close to 0 and scale independence exceeding 0.85 (Fig. 1A). We

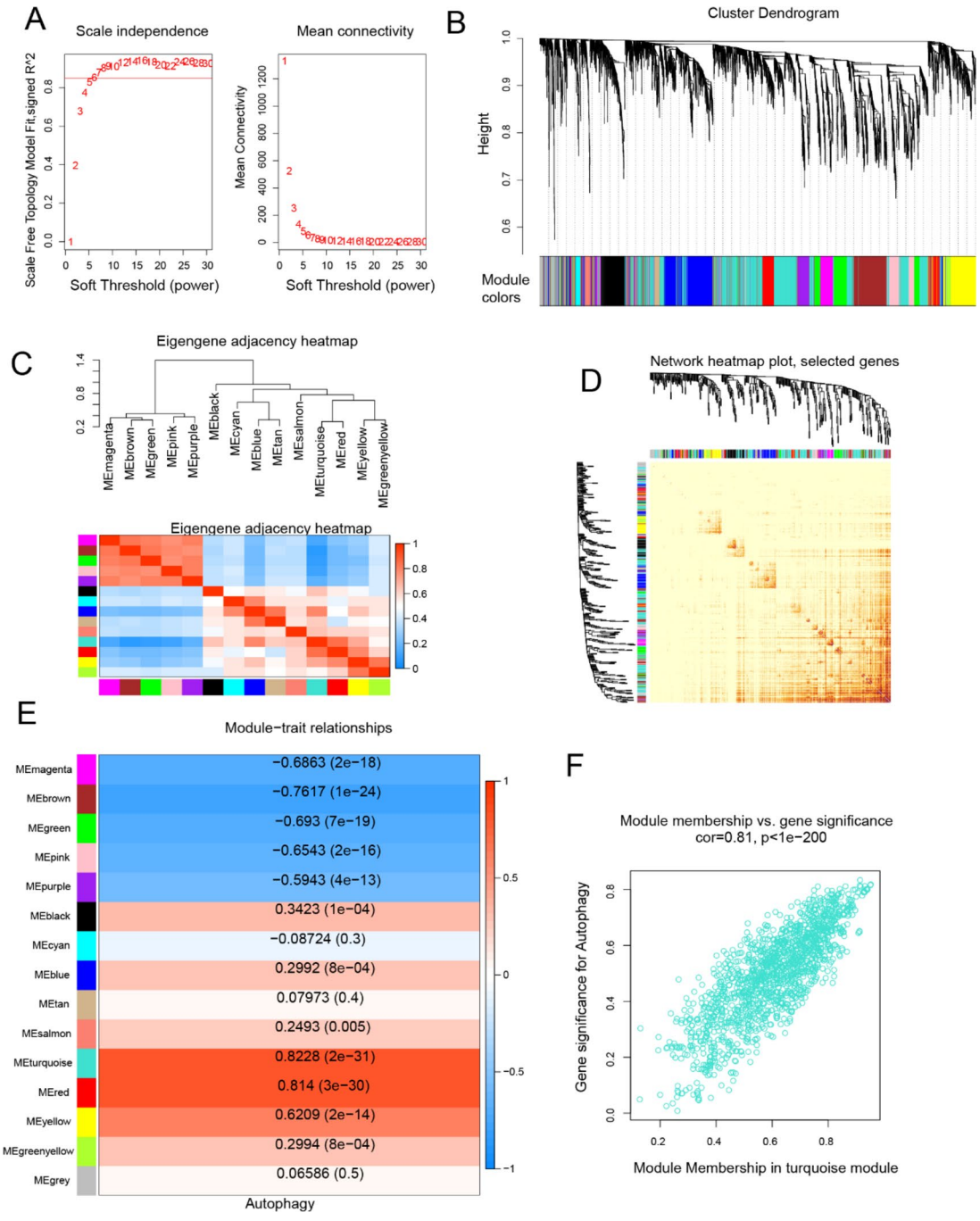

Fig. 1. WGCNA and identification of autophagy-related modules: (**A**) Network topology under various soft threshold powers. (**B**) The genes were divided into different modules via hierarchical clustering. (**C**) Module Relationships: Hierarchical clustering and correlation heatmap of modules, displaying positive correlations in red and negative correlations in blue. (**D**) Topological overlap: Heatmap indicating topological overlap between genes, with lighter colors indicating lower topological overlap and gradually darker red colors indicating greater topological overlap. (**E**) Association between modules and autophagy-related genes, with color-coded correlations. (**F**) MM-GS correlation: Correlation between module membership (MM) and gene significance (GS) for autophagy-related genes in the turquoise module (Cor: absolute correlation coefficient between GS and MM).

proceeded to identify 14 co-expression modules and assigned unrelated genes to the gray module, which was excluded from subsequent analyses (Fig. 1B).

Module eigengene (ME) correlations were computed, and a dendrogram was drawn along with a heatmap to explore module relevance (Fig. 1C). The TOM heatmap was utilized to assess the topological overlap in the gene network (Fig. 1D). We subsequently evaluated the correlation between the 14 MEs and autophagy. Our analysis revealed that genes clustered in the turquoise module ($n = 1421$) exhibited the strongest positive correlation with autophagy ($r = 0.82$, $P < 0.05$; Fig. 1E). Consequently, our focus shifted primarily to genes in the turquoise module for subsequent analyses. A scatter plot illustrating gene significance (GS) and module membership (MM) within the turquoise module demonstrated a highly significant positive correlation between GS and MM ($r = 0.81$, $P < 0.05$; Fig. 1F). This finding indicates a close association between genes in the turquoise module and autophagy.

DEGs associated with sepsis-induced ARDS

Compared with the sepsis-alone group, the sepsis-induced ARDS group presented 13 upregulated DEGs and 43 downregulated genes ($P < 0.05$, |log2-fold change| > 0.5; Fig. 2A). The top five upregulated DEGs (EXT1, COL9A2, RNF10, MAOA, and TMCC2) and the top five downregulated genes (CCL5, CX3CR1, F13A1, M6PR, and CDK2AP1) were visualized via a heatmap and compared between the two groups (Fig. 2B).

By intersecting the DEGs with the genes in the turquoise module, we identified 18 autophagy-related DEGs (Fig. 2C, D).

Diagnostic value of the hub genes

To assess the diagnostic potential of the hub genes, we conducted a ROC curve analysis. The results demonstrated that all 18 genes exhibited discriminatory power, with an AUC > 0.6, indicating that they could serve as potential biomarkers for sepsis-induced ARDS (Fig. 3).

GO and KEGG analysis

To explore the biological functions of the autophagy-related DEGs, we conducted GO and KEGG analyses. Significant enrichment of GO terms was observed across two functional domains (Fig. 4A, B). Within cellular

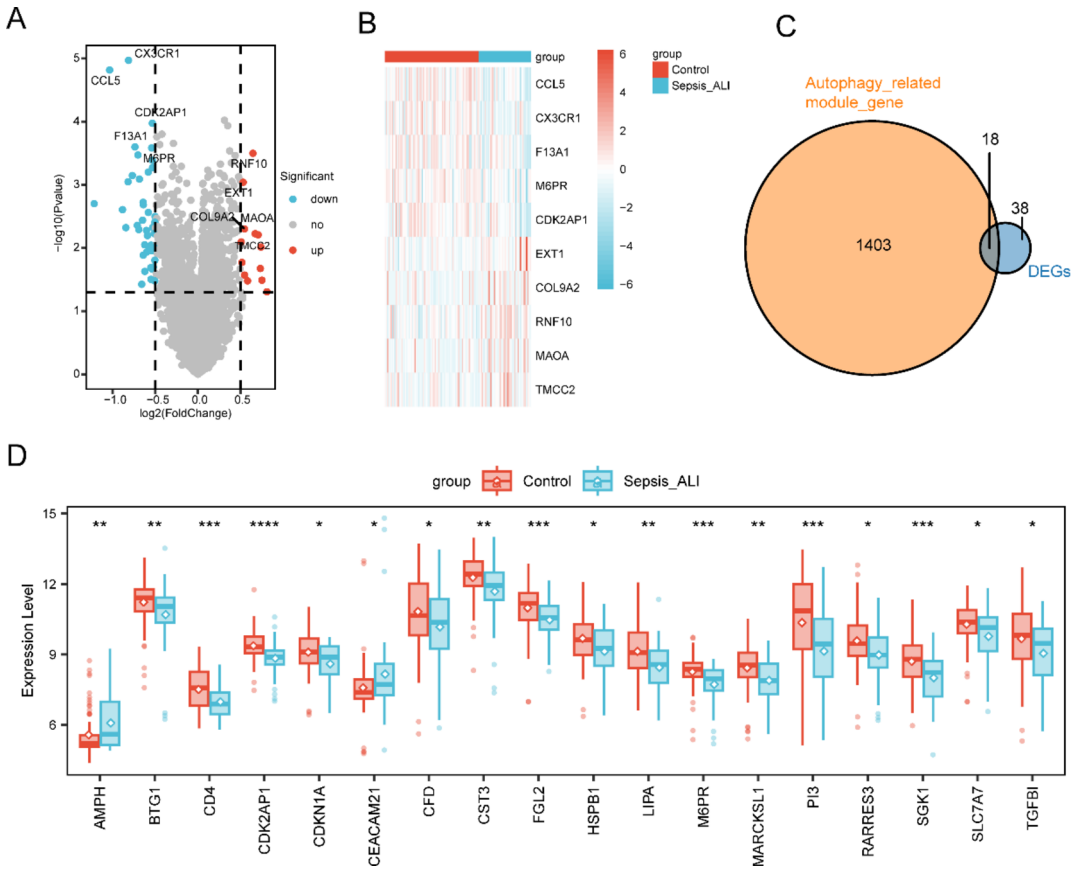

Fig. 2. DEGs in Sepsis-Induced ARDS: (**A**) Volcano plot of DEGs between the sepsis-induced ARDS group and the control group. (**B**) Heatmap displaying the top 5 upregulated and 5 downregulated DEGs. (**C**) Venn diagram illustrating the intersection between autophagy-related genes and DEGs. (**D**) Boxplots depicting 18 autophagy-related DEGs whose expression differed between the two groups. $^{*}P < 0.05$, $^{**}P < 0.01$, $^{***}P < 0.001$, $^{****}P < 0.0001$.

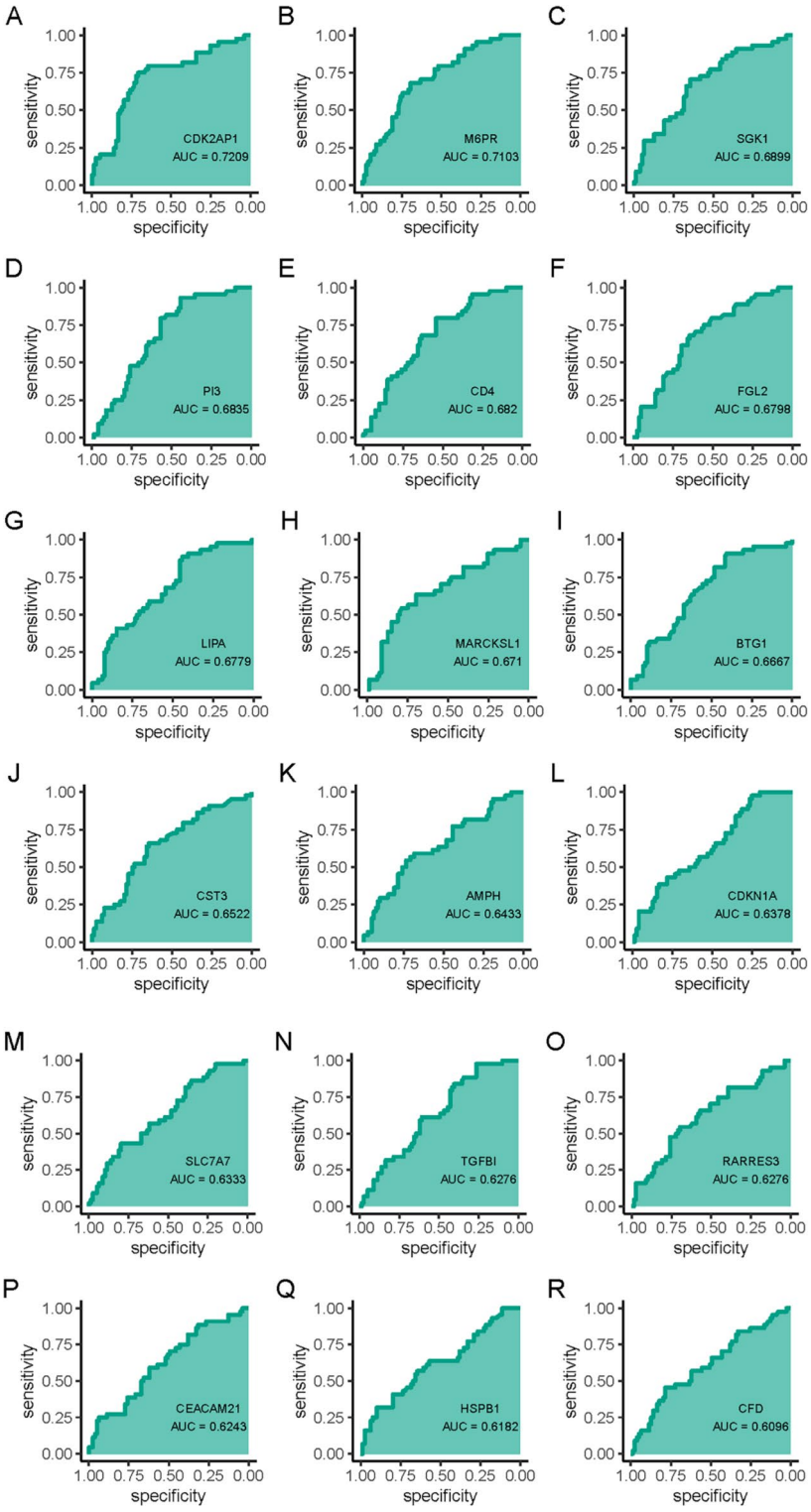

Fig. 3. ROC curves of the hub genes (**A**) CDK2AP1, (**B**) M6PR, (**C**) SGK 1, (**D**) PI3, (**E**) CD4, (**F**) FGL2, (**G**) LIPA, (**H**) MARCKSL1, (**I**) BTG1, (**J**) CST3, (**K**) AMPH, (**L**) CDKN1A, (**M**) SLC7A7, (**N**) TGFBI, (**O**) RARRES3, (**P**) CEACAM21, (**Q**) HSPB1, (**R**) CFD.

components (CC), prominent terms included ficolin-1-rich granule lumen (GO:1904813), ficolin-1-rich granule (GO:0101002), and clathrin-coated endocytic vesicle membrane (GO:0030669). Within molecular function (MF), prominent terms included protein serine/threonine kinase inhibitor activity (GO:0030291), protein kinase inhibition (GO:0004860), and extracellular matrix structural constituent (GO:0005201).However, no

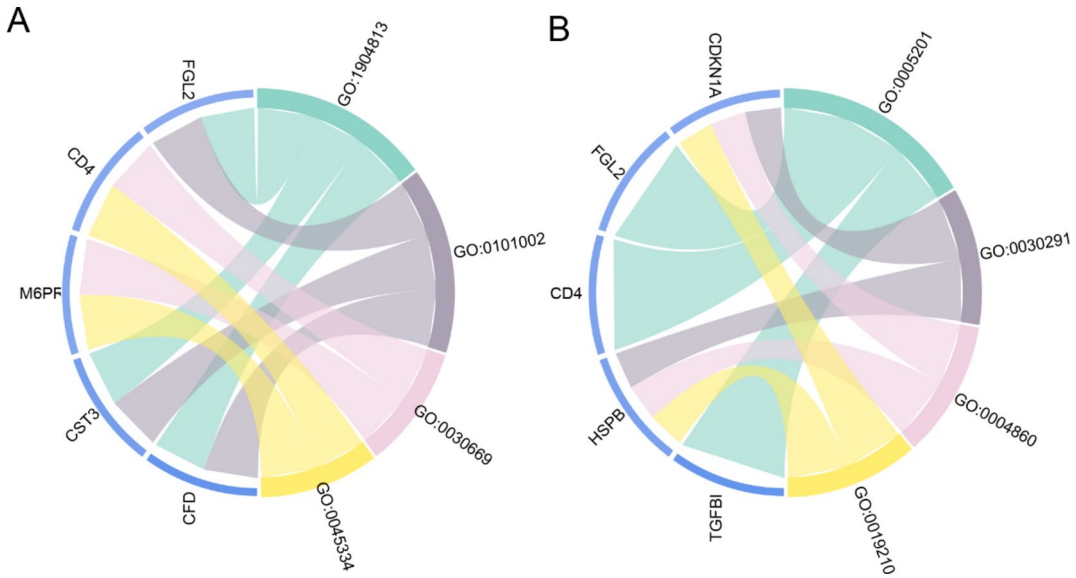

Fig. 4. GO enrichment analysis of autophagy-related DEGs. (**A**) GO terms related to Cellular Component (CC) and associated gene string map. (**B**) GO terms related to Molecular Function (MF) and associated gene string map.

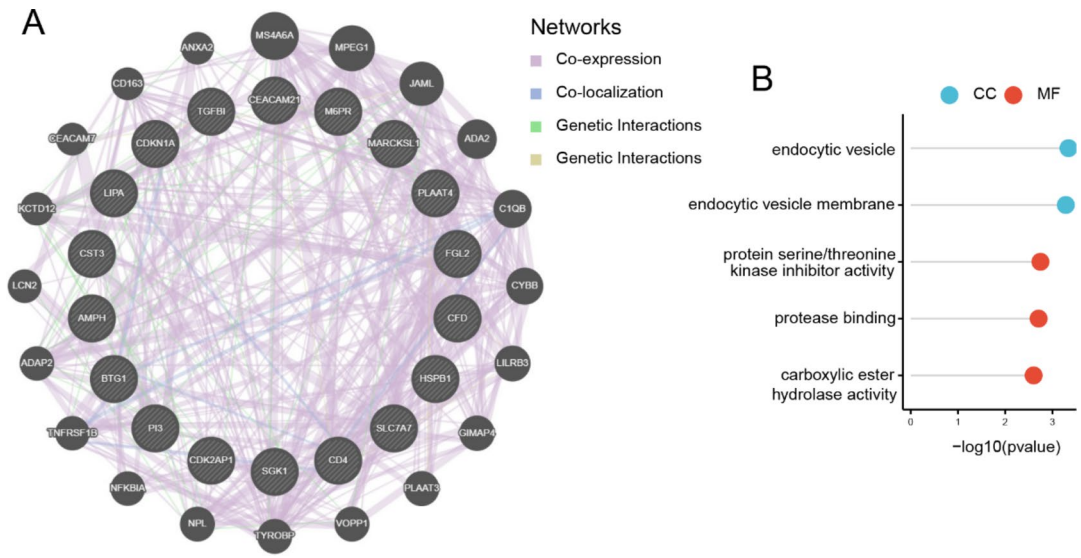

Fig. 5. Functional analysis of hub genes: (**A**) Gene coexpression network diagram; (**B**) GO analysis of coexpressed genes.

biological process (BP) terms or KEGG pathways were found to be enriched. (The detailed GO enrichment results are in Supplementary Material 2)

Gene interaction analysis of hub genes

To comprehensively characterize functional partnerships of the 18 hub genes (full list: CDK2AP1, M6PR, SGK1, PI3, CD4, FGL2, LIPA, MARCKSL1, BTG1, CST3, AMPH, CDKN1A, SLC7A7, TGFBI, RARRES3, CEACAM21, HSPB1, CFD), we employed GeneMANIA platform to construct PPI networks. This analysis revealed 20 genes showing strongest interactions with the hub genes, suggesting their collective involvement in ARDS development (Fig. 5A). For a comprehensive understanding of the functions of signature genes, we selected 18 hub genes and 20 associated genes for GO analysis. The GO enrichment results revealed two distinct functional clusters: endocytic vesicles (GO:0030139) and endocytic vesicle membranes (GO:0030666) in CC, and protein serine/threonine kinase activity (GO:0030291), protease binding (GO:0002020), and carboxylic ester hydrolase activity (GO:0052689) in MF(Fig. 5B).

Comparison of HALLMARK signaling pathways

We initially examined the disparities in 50 HALLMARK signaling pathways between the two groups. Notably, we observed significant downregulation of four pathways in the sepsis-induced ARDS group: HALLMARK APOPTOSIS, HALLMARK COMPLEMENT, HALLMARK IL-2 STAT5 SIGNALING, and HALLMARK KRAS SIGNALING UP (Fig. 6A).

Furthermore, we conducted a correlation analysis between the top five autophagy-related DEGs and the 50 hallmark signaling pathways. SGK1 exhibited broad-spectrum positive correlations with all four downregulated pathways, while CDK2AP1 specifically aligned with HALLMARK KRAS SIGNALING UP. M6PR demonstrated associations with HALLMARK APOPTOSIS, HALLMARK COMPLEMENT, and HALLMARK IL-2 STAT5 SIGNALING. LIPA showed association with HALLMARK KRAS SIGNALING UP, HALLMARK IL-2 STAT5 SIGNALING, and HALLMARK COMPLEMENT. However, CD4 expression showed no significant interaction with the four downregulated pathways (Fig. 6B).

Immune infiltration

Immune cell infiltration likely plays a critical role in the pathogenesis of sepsis-induced ARDS. Using ssGSEA analysis, we identified significant variations in 7 out of 28 immune cell types between groups ($P<0.05$), including activated CD8 T cells, central memory CD4 T cells, effector memory CD8 T cells, myeloid-derived suppressor cells (MDSCs), natural killer (NK) cells, T follicular helper (Tfh) cells, and type 1 T helper (Th1) cells ($P<0.05$) (Fig. 7A). Notably, the sepsis-induced ARDS group exhibited globally distinct immune infiltration compared with controls (Fig. 7B).

Correlation analyses revealed specific interactions between hub genes and immune subsets: BTG1 was significantly correlated with central memory CD4 T cells ($r=0.782$, $P<0.001$) (Fig. 7C), and SLC7A7 was significantly correlated with MDSCs ($r=0.747$, $P<0.001$) (Fig. 7D). The correlation of immune cell infiltration revealed positive inter-correlations among most immune cells (Fig. 7E), suggesting coordinated immune network activation in sepsis-induced ARDS.

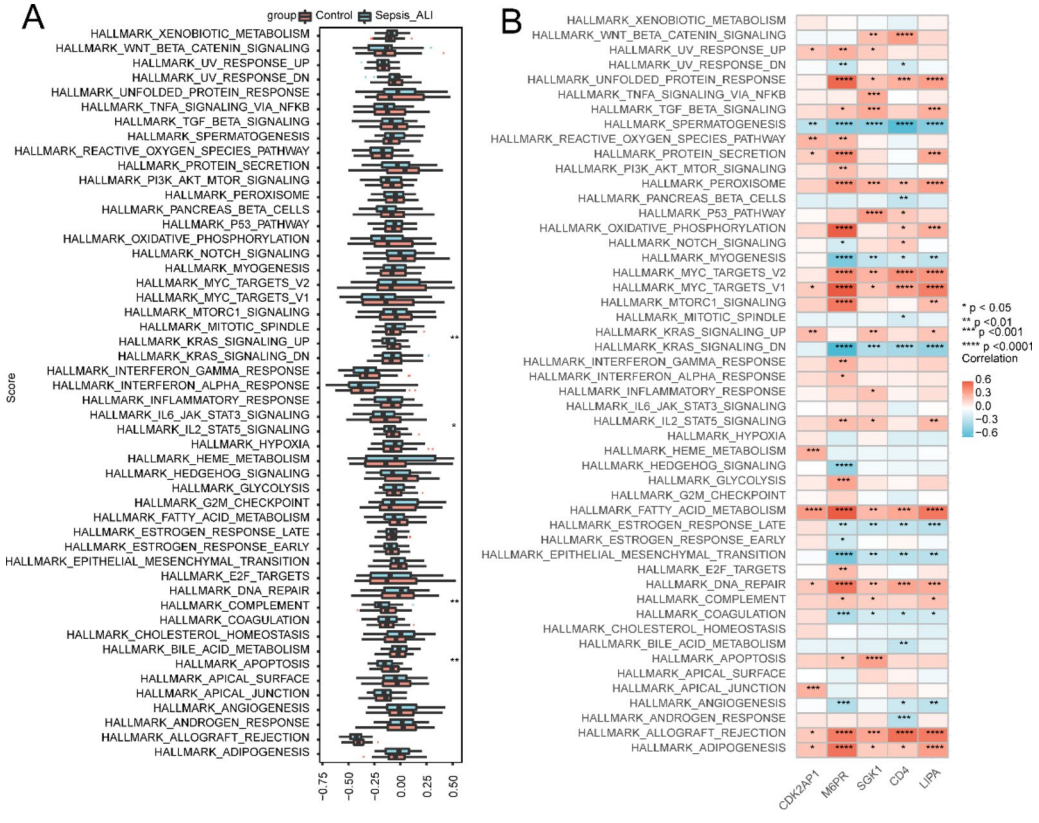

Fig. 6. Correlations of HALLMARK signaling pathways with autophagy-related hub genes in sepsis-induced ARDS. (**A**) Comparative analysis of 50 HALLMARK signaling pathways between sepsis-induced ARDS and control groups. Four pathways—HALLMARK APOPTOSIS, HALLMARK COMPLEMENT, HALLMARK IL-2 STAT5 SIGNALING, and HALLMARK KRAS SIGNALING UP—were significantly downregulated in the sepsis-induced ARDS group. (**B**) Correlation network between top five autophagy-related DEGs and HALLMARK Signaling Pathways. ****$P<0.0001$, ***$P<0.001$, **$P<0.01$, *$P<0.05$.

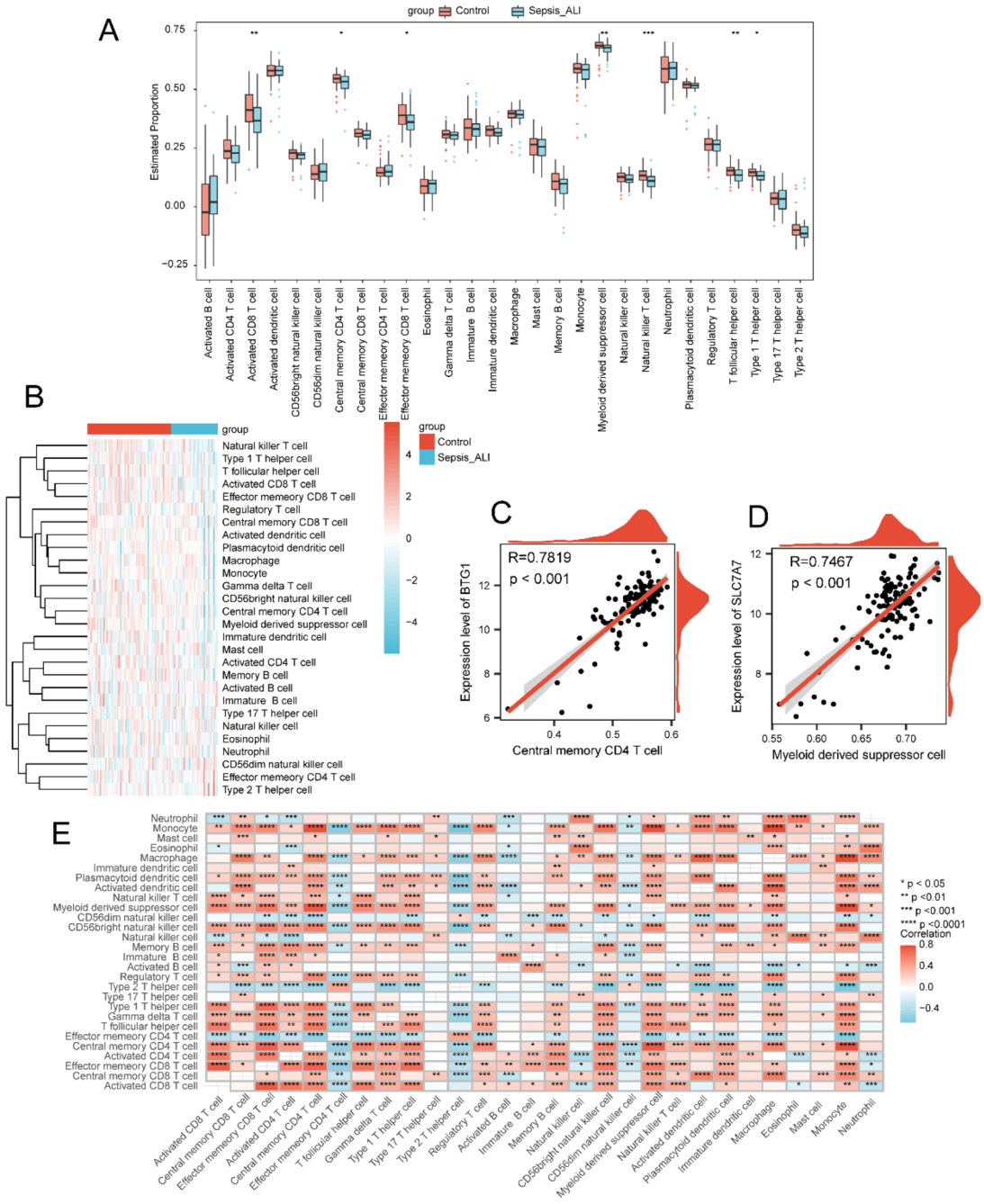

Fig. 7. Immune landscape characterization in sepsis-induced ARDS. (**A**) Differential immune cell infiltration. CIBERSORT analysis revealed significant abundance differences ($P < 0.05$) in 7 immune subsets: activated CD8 T cells, central memory CD4 T cells, effector memory CD8 T cells, MDSCs, NK cells, Tfh cells, and Th1 cells. (**B**) Heatmap illustrating the overall level of immune cell infiltration across both groups, reflecting systemic immune response engagement. (**C**) BTG1 expression strongly correlates with central memory CD4 T cells abundance ($r = 0.782$, $P < 0.001$). (**D**) SLC7A7 shows significant association with MDSCs ($r = 0.747$, $P < 0.001$). (**E**) Immune network coordination. Correlation matrix reveals predominant positive associations (red) among immune cell types, highlighting synchronized immune activation in sepsis-induced ARDS. $^{****}P < 0.0001$, $^{***}P < 0.001$, $^{**}P < 0.01$, $^{*}P < 0.05$.

Hub gene expression in beas-2B cells

Out of a total of 18 hub genes, 6 genes exhibited downregulation in Beas-2B cells when treated with LPS compared to untreated group (Fig. 8). The remaining 12 hub genes showed no significant difference between the two groups or did not demonstrate notable expression in either group.

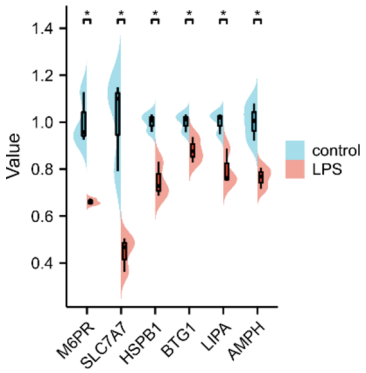

Fig. 8. Six out of 18 candidate hub genes showed significant downregulation in LPS-treated Beas-2B cells compared to untreated controls.

Discussion

In this study, we identified 18 downregulated autophagy-related hub genes in sepsis-induced ARDS through comprehensive bioinformatics analysis. All of these hub genes exhibited significant diagnostic potential for sepsis-induced ARDS, highlighting the involvement of autophagy in the pathogenesis of this condition. Additionally, we observed a significant downregulation of 6 out of the 18 hub genes in LPS-treated Beas-2B cells. This finding suggests that autophagy may contribute to the disruption of the pulmonary alveolar capillary barrier in ARDS.

GO enrichment and PPI analysis revealed that the autophagy-related hub genes are associated with endocytosis (GO: 0030669, GO: 0030139 and GO: 0030666) and protein kinase inhibitor activity (GO: 0030291 and GO: 0004860). Autophagy and endocytosis are membrane-vesicle cellular pathways responsible for the degradation and recycling of intracellular and extracellular components, respectively[19]. A growing body of evidence indicates a mutual dependence between autophagy and endocytosis[20]. Protein kinases are enzymes that regulate various cellular processes, affecting signaling pathways implicated in inflammation[21]. Several kinases have been studied for their potential as therapeutic targets in ARDS, including p38 Mitogen-Activated Protein Kinase (MAPK)[22], c-Jun N-terminal Kinase (JNK)[23], Protein Kinase B (Akt)[24], and Rho-Associated Protein Kinase (ROCK)[25] etc. These findings suggest that autophagy may modulate ARDS progression via kinase activity regulation. Another intriguing finding is that the autophagy-related DEGs are closely related to Ficolin-1-rich granule (GO: 1904813 and GO: 0101002). Ficolin-1-rich granule is a type of neutrophil granules with enigmatic functions[26]. While no direct evidence exists linking Ficolin-1 to ARDS, its homolog Ficolin-2 demonstrates clinical relevance: as a complement lectin regulating pathogen recognition and immune responses[27], decreased serum levels predict neonatal ARDS severity[28]. Considering the role of Ficolin-2 in ARDS, we can speculate that Ficolin-1 may also play a certain role in the pathological process of ARDS, particularly in immune response and inflammation regulation. However, the initial findings regarding Ficolin-1's role in sepsis-induced ARDS are preliminary and require further validation beyond bioinformatics approaches.

We identified four significantly downregulated Hallmark signaling pathways in the sepsis-induced ARDS group: apoptosis, complement, IL-2/STAT5 signaling, and KRAS signaling. The apoptosis pathway exhibited cell-type-specific dysregulation, characterized by apoptotic resistance in neutrophils while accelerated death in epithelial and endothelial cells[29], suggesting its dual role in ARDS pathogenesis. Dysregulated activation of the complement cascade may also contribute to the pathological processes of ARDS, holding significant potential for therapeutic intervention in ARDS[30]. The IL-2/STAT5 signaling pathway is a crucial immune signaling pathway that regulates T-cell proliferation, differentiation, survival, and activation, thereby influencing the immune response[31]; its enrichment in peripheral blood monocytes correlated with poor outcomes, whereas alveolar macrophage activation was associated with a favorable prognosis[31,32]. This cellular compartmentalization highlights critical limitations in extrapolating peripheral immune signatures to alveolar pathophysiology. The relationship between KRAS signaling and ARDS has not yet been clearly established. Additionally, we found that SGK1, CDK2AP1, M6PR, and LIPA were correlated with these four pathways, all showing positive correlations. This correlation suggests a link between the low expression of these genes and the onset of ARDS, indicating that the downregulation of autophagy-regulated genes SGK1, CDK2AP1, M6PR, and LIPA may promote the development of ARDS through the inhibition of these specific pathways.

Immune dysfunction constitutes a critical pathophysiological link between ARDS and sepsis. Our comparative immune infiltration analysis revealed significant depletion of seven immune cell subsets in sepsis-induced ARDS compared to sepsis controls. Notably, the diminished activated and effector memory CD8 + T cell populations (crucial for viral clearance) may impair pulmonary pathogen control[33], while the reduced central memory CD4 + T cells could compromise adaptive immune memory and secondary response efficacy to infection[34]. MDSCs regulate immune responses in ARDS by inhibiting T cell activity and acute inflammation, aiding repair and improving lung disease symptoms[35]. A decrease in NK cells may impair the immune function and clearance of infection in ARDS patients[36]. Tfh cells play a central role in the activation of B cells and the promotion of antibody production[12]; whereas Th1 cells influence cellular immune responses[37]. A decrease in Tfh or Th1 cells may also compromise the lungs' capacity to control infections[12,37]. The correlation between central

memory CD4 + T cells and BTG1, as well as MDSCs and SLC7A7, suggests that these autophagy-related genes may play a regulatory role in the immune environment associated with ARDS.

The genome expression in the two datasets utilized in this study originated from whole blood, rendering it indistinguishable as to the source of variation. Given that diffuse alveolar damage is a characteristic feature of ARDS, we investigated the expression of 18 hub genes in Beas-2B cells, an epithelial cell line, treated with or without LPS. Six out of the 18 hub genes exhibited significant downregulation in the Beas-2B cells treated with LPS, namely SLC7A7, BTG1, HSPB1, M6PR, LIPA and AMPH. SLC7A7 demonstrates a significant correlation with MDSCs, acting as a brake to restrain inflammation[38]. BTG1 is a member of an antiproliferative gene family, serving as a regulator of apoptosis[39]. HSPB1 can increase cell sensitivity to ferroptosis, facilitating ARDS development[40]. M6PR is a receptor found on the surface of cells that plays a role in the trafficking and targeting of certain proteins within cells[41–43]. We postulate the expression difference of AMPH may act through its impact on the cell membrane shaping, which plays important roles in a wide variety of cellular processes, including secretion and endocytosis, etc[44]. Pulmonary surfactant consists of 90–95% lipids and 5–10% surfactant proteins (SP), and lysosomal acid lipase (encoded by LIPA) deficiency could cause respiratory inflammation and destruction in the lung[45].

Classical biomarkers like C-reactive protein (CRP), procalcitonin (PCT), and interleukin-6 (IL-6) indicate systemic inflammation[46] but lack ARDS specificity and may not reflect disease severity[47], emphasizing the need for precise diagnostics. Integrating multiple biomarkers into diagnostic protocols could enhance ARDS diagnosis and treatment. And this study highlights the importance of autophagy-related genes in sepsis-induced ARDS as potential novel biomarkers and therapeutic targets.

The present study has several limitations. Firstly, the reliance on only two GEO transcriptome datasets limits the diversity and representativeness of the data. Secondly, sample heterogeneity complicates both analytical rigor and biological interpretation. Additionally, our experimental validation is limited; we have conducted qPCR validation exclusively in Beas-2B cells. Further in vivo and clinical studies are necessary to enhance the reliability and clinical relevance of our findings. Finally, key mechanistic insights—such as the downregulation of pathways (apoptosis, complement, IL-2/STAT5 signaling, KRAS), Ficolin-1's role in sepsis-induced ARDS, etc.—require experimental validation beyond computational analyses.

Despite these limitations, our results provide valuable insights that could be translated into clinical practice, particularly in diagnostics using the hub genes identified in this study and in treatments targeting autophagy-related pathways or immune cell infiltration.

In summary, this research addresses a critical gap in the understanding of the molecular mechanisms of sepsis-induced ARDS by focusing on the role of autophagy-related genes. Through the application of advanced bioinformatics techniques, we provide new insights into the pathogenesis of this condition and identify potential biomarkers for early diagnosis and targeted therapy, paving the way for future studies and clinical applications.

Data availability

The datasets analysed during the current study are publicly available through GEO (https://www.ncbi.nlm.nih.gov/geo/query/acc.cgi?acc=GSE10474 and https://www.ncbi.nlm.nih.gov/geo/query/acc.cgi?acc=GSE32707).

Received: 8 August 2024; Accepted: 27 February 2025
Published online: 06 March 2025

References

1. Singer, M. et al. The third international consensus definitions for sepsis and septic shock (Sepsis-3). *JAMA* **315** (8), 801–810 (2016).
2. Mikkelsen, M. E. et al. The epidemiology of acute respiratory distress syndrome in patients presenting to the emergency department with severe sepsis. *Shock* **40** (5), 375–381 (2013).
3. Iriyama, H. et al. Risk modifiers of acute respiratory distress syndrome in patients with non-pulmonary sepsis: a retrospective analysis of the FORECAST study. *J. Intens. Care.* **8**, 7 (2020).
4. Li, S. et al. Prevalence, potential risk factors and mortality rates of acute respiratory distress syndrome in Chinese patients with sepsis. *J. Int. Med. Res.* **48** (2), 300060519895659 (2020).
5. Nam, H. et al. Nonpulmonary risk factors of acute respiratory distress syndrome in patients with septic bacteraemia. *Korean J. Intern. Med.* **34** (1), 116–124 (2019).
6. Seethala, R. R. et al. Early risk factors and the role of fluid administration in developing acute respiratory distress syndrome in septic patients. *Ann. Intens. Care.* **7** (1), 11 (2017).
7. Shi, Y., Wang, L., Yu, S., Ma, X. & Li, X. Risk factors for acute respiratory distress syndrome in sepsis patients: a retrospective study from a tertiary hospital in China. *BMC Pulm. Med.* **22** (1), 238 (2022).
8. Xu, C., Zheng, L., Jiang, Y. & Jin, L. A prediction model for predicting the risk of acute respiratory distress syndrome in sepsis patients: a retrospective cohort study. *BMC Pulm. Med.* **23** (1), 78 (2023).
9. Matthay, M. A. et al. Acute respiratory distress syndrome. *Nat. Rev. Dis. Primers* **5** (1), 18 (2019).
10. Lelubre, C. & Vincent, J. L. Mechanisms and treatment of organ failure in sepsis. *Nat. Rev. Nephrol.* **14** (7), 417–427 (2018).
11. Liu, C., Xiao, K. & Xie, L. Progress in preclinical studies of macrophage autophagy in the regulation of ALI/ARDS. *Front. Immunol.* **13**, 922702 (2022).
12. Sun, M., Yang, Q., Hu, C., Zhang, H. & Xing, L. Identification and validation of autophagy-related genes in sepsis-induced acute respiratory distress syndrome and immune infiltration. *J. Inflamm. Res.* **15**, 2199–2212 (2022).
13. Zhu, D. et al. The downregulation of miR-129-5p relieves the inflammatory response in acute respiratory distress syndrome by regulating PPARgamma-mediated autophagy. *Ann. Transl. Med.* **10** (6), 345 (2022).
14. Dong, J. et al. Acute lung injury: a view from the perspective of necroptosis. *Inflamm. Res.* **73** (6), 997–1018 (2024).
15. Lei, M. et al. Different intensity of autophagy regulate interleukin-33 to control the uncontrolled inflammation of acute lung injury. *Inflamm. Res.* **68** (8), 665–675 (2019).
16. Mizushima, N. Autophagy: process and function. *Genes Dev.* **21** (22), 2861–2873 (2007).
17. Levine, B., Mizushima, N. & Virgin, H. W. Autophagy in immunity and inflammation. *Nature* **469** (7330), 323–335 (2011).
18. Li, Z. Y. et al. Autophagy as a double-edged sword in pulmonary epithelial injury: a review and perspective. *Am. J. Physiol. Lung Cell. Mol. Physiol.* **313** (2), L207–L217 (2017).

19. Takei, K. & Haucke, V. Clathrin-mediated endocytosis: membrane factors pull the trigger. *Trends Cell. Biol.* **11** (9), 385–391 (2001).
20. Birgisdottir, A. B. & Johansen, T. Autophagy and endocytosis—Interconnections and interdependencies. *J. Cell. Sci.* **133** (10), 1 (2020).
21. Zarrin, A. A., Bao, K., Lupardus, P. & Vucic, D. Kinase Inhibition in autoimmunity and inflammation. *Nat. Rev. Drug Discov.* **20** (1), 39–63 (2021).
22. Christie, J. D. et al. A randomized dose-escalation study of the safety and anti-inflammatory activity of the p38 mitogen-activated protein kinase inhibitor dilmapimod in severe trauma subjects at risk for acute respiratory distress syndrome. *Crit. Care Med.* **43** (9), 1859–1869 (2015).
23. Spinelli, F. R., Conti, F. & Gadina, M. HiJAKing SARS-CoV-2? The potential role of JAK inhibitors in the management of COVID-19. *Sci. Immunol.* **5** (47), 1 (2020).
24. Li, L. F., Liao, S. K., Huang, C. C., Hung, M. J. & Quinn, D. A. Serine/threonine kinase-protein kinase B and extracellular signal-regulated kinase regulate ventilator-induced pulmonary fibrosis after bleomycin-induced acute lung injury: a prospective, controlled animal experiment. *Crit. Care.* **12** (4), R103 (2008).
25. Abedi, F., Hayes, A. W., Reiter, R. & Karimi, G. Acute lung injury: the therapeutic role of Rho kinase inhibitors. *Pharmacol. Res.* **155**, 104736 (2020).
26. Othman, A., Sekheri, M. & Filep, J. G. Roles of neutrophil granule proteins in orchestrating inflammation and immunity. *FEBS J.* **289** (14), 3932–3953 (2022).
27. Zhu, L. W. et al. Ficolin-A induces macrophage polarization to a novel pro-inflammatory phenotype distinct from classical M1. *Cell. Commun. Signal.* **22** (1), 271 (2024).
28. Gajek, G. et al. Association of low ficolin-2 concentration in cord serum with respiratory distress syndrome in preterm newborns. *Front. Immunol.* **14**, 1107063 (2023).
29. Sauler, M., Bazan, I. S. & Lee, P. J. Cell death in the lung: the apoptosis-necroptosis axis. *Annu. Rev. Physiol.* **81**, 375–402 (2019).
30. Yang, Z., Nicholson, S. E., Cancio, T. S., Cancio, L. C. & Li, Y. Complement as a vital nexus of the Pathobiological connectome for acute respiratory distress syndrome: an emerging therapeutic target. *Front. Immunol.* **14**, 1100461 (2023).
31. Ye, C., Brand, D. & Zheng, S. G. Targeting IL-2: an unexpected effect in treating immunological diseases. *Signal. Transduct. Target. Ther.* **3**, 2 (2018).
32. Morrell, E. D. et al. Peripheral and alveolar cell transcriptional programs are distinct in acute respiratory distress syndrome. *Am. J. Respir Crit. Care Med.* **197** (4), 528–532 (2018).
33. Yan, L., Chen, Y., Han, Y. & Tong, C. Role of CD8(+) T cell exhaustion in the progression and prognosis of acute respiratory distress syndrome induced by sepsis: a prospective observational study. *BMC Emerg. Med.* **22** (1), 182 (2022).
34. Chevalier, N. et al. CXCR5 expressing human central memory CD4 T cells and their relevance for humoral immune responses. *J. Immunol.* **186** (10), 5556–5568 (2011).
35. Zhang, M. N., Yuan, Y. L. & Ao, S. H. Advances in the study of myeloid-derived suppressor cells in infectious lung diseases. *Front. Immunol.* **14**, 1125737 (2023).
36. Park, K. J. et al. Deficiency and dysfunctional roles of natural killer T cells in patients with ARDS. *Front. Immunol.* **15**, 1433028 (2024).
37. Mitsuyama, Y. et al. T cell dysfunction in elderly ARDS patients based on MiRNA and mRNA integration analysis. *Front. Immunol.* **15**, 1368446 (2024).
38. Rotoli, B. M. et al. Downregulation of SLC7A7 triggers an inflammatory phenotype in human macrophages and airway epithelial cells. *Front. Immunol.* **9**, 508 (2018).
39. Lee, H. et al. Role of antiproliferative B cell translocation gene-1 as an apoptotic sensitizer in activation-induced cell death of brain microglia. *J. Immunol.* **171** (11), 5802–5811 (2003).
40. Qu, M. et al. The role of ferroptosis in acute respiratory distress syndrome. *Front. Med.* **8**, 651552 (2021).
41. Bonifacino, J. S. & Rojas, R. Retrograde transport from endosomes to the trans-Golgi network. *Nat. Rev. Mol. Cell. Biol.* **7** (8), 568–579 (2006).
42. Pfeffer, S. R. Multiple routes of protein transport from endosomes to the trans golgi network. *FEBS Lett.* **583** (23), 3811–3816 (2009).
43. Banik, S. M. et al. Lysosome-targeting chimaeras for degradation of extracellular proteins. *Nature* **584** (7820), 291–297 (2020).
44. Rao, Y. & Haucke, V. Membrane shaping by the Bin/amphiphysin/Rvs (BAR) domain protein superfamily. *Cell. Mol. Life Sci.* **68** (24), 3983–3993 (2011).
45. Lian, X., Yan, C., Yang, L., Xu, Y. & Du, H. Lysosomal acid lipase deficiency causes respiratory inflammation and destruction in the lung. *Am. J. Physiol. Lung Cell. Mol. Physiol.* **286** (4), L801–807 (2004).
46. Terpstra, M. L., Aman, J., van Nieuw Amerongen, G. P. & Groeneveld, A. B. Plasma biomarkers for acute respiratory distress syndrome: a systematic review and meta-analysis. *Crit. Care Med.* **42** (3), 691–700 (2014).
47. van der Zee, P., Rietdijk, W., Somhorst, P., Endeman, H. & Gommers, D. A systematic review of biomarkers multivariately associated with acute respiratory distress syndrome development and mortality. *Crit. Care.* **24** (1), 243 (2020).

Acknowledgements

We would like to express our gratitude for the support provided by the library of Zhejiang University during the course of this research.

Author contributions

W.W. made the conception and wrote the main manuscript. W.W., Z.J., and L.H. completed the bioinformatics analysis. H.D. completed the qPCR. L.Z. and F.S. supervised the study and edited the manuscript. All authors reviewed the manuscript.

Declarations

Competing interests

The authors declare no competing interests.

Ethical approval and consent to participate

The Ethics Committee of the First Affiliated Hospital, Zhejiang University School of Medicine waived the requirement for ethics approval and consent to participate in this study because it does not involve human subjects, live animals, or sensitive data processing that would typically require ethical oversight.

Additional information

Supplementary Information The online version contains supplementary material available at https://doi.org/10.1038/s41598-025-92409-7.

Correspondence and requests for materials should be addressed to S.F. or Z.L.

Reprints and permissions information is available at www.nature.com/reprints.

Publisher's note Springer Nature remains neutral with regard to jurisdictional claims in published maps and institutional affiliations.